Construction and Building Materials 416 (2024) 135225

Contents lists available at ScienceDirect

Construction and Building Materials

journal homepage: www.elsevier.com/locate/conbuildmat

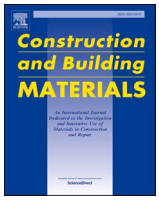

Evaluation on performance of rubber tire powder and waste glass modified binder as crack filling materials using 3D printing technology

Tam Minh Phan, Hye-Ju Ma, Dae-Wook Park *

Department of Civil and Environmental Engineering, Kunsan National University, Gunsan, Jeonbuk 54150, Republic of Korea

ARTICLE INFO

Keywords:
Asphalt pavement
3D Printing
Crack Filling
Rubber Tire Powder
Waste Glass

ABSTRACT

This study investigates the potential use of waste materials, specifically rubber tire powder (RTP) and waste glass, as substitutes for asphalt binder in pavement crack sealing via three-dimensional (3D) printing. It aims to reduce binder consumption by utilizing these waste materials as printing materials and determine the optimum waste material content within the modified asphalt binder. Assessing crack-filled sample performance by various tests such as semi-circular bending and four-point bending evaluates the effect of 3D crack sealing under monotonic and repeated loads. The research findings showed several key enhancements: crack-filled samples exhibited improved indirect tensile strength (ITS) by up to 42 % compared to unfilled control samples. Notably, specific compositions as PG64–22 with 10 % waste glass or 20 % rubber tire powder achieved higher ITS compared to that of modified with PG58–22 binder. These crack-filled samples also displayed improved ductile behavior, approximately doubling the deformation at peak load compared to unfilled samples. Enhanced fracture energy values, about three times as high as those of unfilled samples. Shear bond strength tests revealed the superiority of PG64–22 binder over PG58–22, with increased shear strength observed in samples containing waste materials. However, limitations exist regarding the concentration of waste materials; utilizing over 40 % rubber tire powder by binder weight at a printing temperature of 120 ℃ was not recommended due to the increase in binder viscosity, while temperature control was necessary to prevent segregation when incorporating high-density materials as waste glass into asphalt binder.

1. Introduction

Asphalt mixtures play a key role in modern transportation infrastructure, offering an excess of advantages such as flexibility, durability, cost-effectiveness, and ease of construction [1,2]. These mixtures provide essential benefits by effectively distributing the loads imposed by vehicles, resisting deformation caused by temperature fluctuations, and offering superior noise reduction and skid resistance. Asphalt pavements, due to their flexibility, can accommodate varying traffic loads and climatic conditions, making them a preferred choice for road surfaces globally [3]. Despite many advantages, asphalt pavements are susceptible to distress over time, mainly due to cracks and potholes. Cracks are a common occurrence in asphalt pavements, arising from various factors including aging, traffic loading, and temperature variations [4]. Under service life, these cracks can significantly compromise the pavement's structural integrity. Moreover, small cracks that are not addressed can evolve into larger structural issues, leading to the formation of potholes [5]. These distresses not only detract from the overall ride quality but also pose safety hazards for motorists and pedestrians. The presence of cracks and potholes accelerates the deterioration of asphalt pavements, reducing their service life and increasing maintenance costs [6]. Water penetration into these cracks exacerbates the problem by weakening the underlying layers of the pavement, ultimately leading to further degradation. Additionally, moisture intrusion combined with freeze-thaw cycles can significantly the distress, accelerating pavement deterioration [7–9]. To address these challenges, ongoing research is focused on innovative strategies for effective crack and pothole repair in asphalt pavements [5,10]. Novel approaches include the use of advanced materials, such as capsules and cold asphalt mixture. Additionally, using technologies like 3D printing for crack filling offer promising solutions to enhance pavement durability and performance [10–12]. These advancements aim to extend the service life of asphalt pavements, thereby reducing maintenance costs and minimizing disruptions to transportation networks.

The integration of 3D printing technology into civil engineering, particularly in the preparation of asphalt pavement, presents a

* Corresponding author.
E-mail address: dpark@kunsan.ac.kr (D.-W. Park).

https://doi.org/10.1016/j.conbuildmat.2024.135225
Received 20 November 2023; Received in revised form 2 January 2024; Accepted 26 January 2024
Available online 3 February 2024

promising potential for innovation and advancement [13]. The 3D printing, also known as additive manufacturing, has gained attention as a transformative technique in civil engineering due to its precision, customization capabilities, and efficiency in material utilization [14]. In the context of asphalt pavement, 3D printing facilitates the precise application of materials for crack sealing and repair, offering a solution to address pavement distresses [15]. The technology enables the deposition of asphalt binder into cracks with precision, effectively sealing and reinforcing the damaged areas. Several studies have indicated that 3D printing for crack filling exhibits promising results in restoring the structural integrity of pavements and mitigating the propagation of cracks, thereby preventing further deterioration [15,16]. Moreover, this method allows for the incorporation of various materials, such as modified binders and waste materials like rubber tire powder, into the printing process, enhancing the overall properties of the repaired sections [11]. Despite its promising potential, challenges such as optimizing printing parameters, ensuring material compatibility, and addressing scale-up issues remain areas of ongoing research and development. In addition, traditional asphalt pavement repair methods predominantly rely on the use of asphalt binders, which can be costly due to material procurement and manufacturing expenses. Furthermore, the environmental impact of excessive asphalt binder usage, including its production-related emissions and reliance on finite resources, raises concerns regarding sustainability and resource conservation. By incorporating waste materials such as waste glass and rubber tire powder as partial replacements for conventional asphalt binders in 3D printing applications, the excessive reliance on costly virgin binders can be mitigated. Furthermore, utilizing the 3D printing method for crack sealing not only minimizes the wastage of sealing materials and labor efforts but also enhances labor safety, especially when conducting sealing activities on highways where vehicles are traveling at high speeds.

Nowadays, the integration of waste materials like waste glass and rubber tire powder into asphalt mixtures has emerged as a sustainable approach with considerable potential to enhance the performance, durability, and environmental sustainability of road construction materials [17,18]. These waste materials, when appropriately processed and incorporated into asphalt mixtures, contribute to improved pavement properties and environmental conservation [19]. Waste glass, typically obtained from recycled bottles and other glass products, can be ground into fine particles and utilized as a supplementary material in asphalt mixtures [20]. Research indicates that waste glass powder, when added to asphalt mixtures, can enhance various mechanical properties of the resulting pavement [21]. It has been found to improve rutting resistance, increase stiffness, and extend the fatigue life of asphalt pavements [22]. Moreover, the use of waste glass in asphalt mixtures not only decreases this material from landfills but also reduces the demand for virgin materials, contributing to resource conservation and sustainable practices in road construction. Similarly, rubber tire powder, derived from recycled tires, has garnered attention as a beneficial additive in asphalt mixtures due to its elastomeric properties [23,24]. Incorporating rubber tire powder in asphalt binders has shown promise in improving the high-temperature performance and storage stability of asphalt mixtures [25]. It contributes to enhanced rutting resistance, reduced temperature susceptibility, and increased fatigue resistance of asphalt pavements, thereby extending their service life [26,27]. Numerous studies have experimented with different proportions of tire powder to modify asphalt binder, aiming to enhance its properties. However, the majority of these studies restricted the tire powder content to a maximum of 30 % by weight of the asphalt binder. Their goal was to modify asphalt binder properties, including improving the binder grade, augmenting the $G^*/\sin\delta$ of rubber-modified asphalt binder, and decreasing binder creep stiffness. Notably, there has been a scarcity of research exploring the utilization of waste glass and rubber tire powder-modified asphalt binder specifically for sealing purposes [28–30]. Gong et al. conducted research on the preparation and enhancement of 3D printed asphalt containing crumb rubber, employing a high mixing temperature of 180 ℃. In their study, the asphalt binder modified with crumb rubber was mixed at 3000 RPM at 180 ℃ for 45 min, resulting in the dissolution of a portion of the crumb rubber and altering the physical characteristics of the asphalt binder [11]. While this method led to potential improvements in the performance of the crumb rubber modified binder, it also escalated the energy required for the binder preparation process. Consequently, challenges persist in effectively integrating waste materials into asphalt mixtures. Ensuring proper blending, compatibility, and determining the optimal dosage of waste materials are crucial factors that require careful consideration. Achieving the desired enhancement in pavement performance while maintaining durability and long-term performance necessitates comprehensive studies and optimization of the incorporation methods.

Therefore, the primary aim of this research is to investigate the feasibility and effectiveness of employing waste materials, specifically waste glass and rubber tire powder, as sustainable substitutes for conventional binders in 3D printing applications dedicated to crack sealing within asphalt pavements. The study focuses on exploring the potential of these waste materials to replace the original binders used for filling asphalt pavement cracks. Various proportions of waste materials, ranging from 10 % to 50 % by weight of binder, were examined. This investigation considered two types of asphalt binder, including PG58–22 and PG64–22. To evaluate the performance, compatibility, and suitability of waste glass and rubber tire powder as filling materials in the 3D printing for crack sealing, a series of tests were conducted. These tests included assessments of mechanical properties, adhesion characteristics, and overall efficacy in crack sealing applications, employing methods such as the semi-circular bending test, shear bond strength test, four-point bending test, and analysis of binder flow rate. In general, this study provides an overview of the utilization of waste glass and rubber tire powder for pavement crack sealing using 3D printing techniques.

2. Materials and asphalt 3D printer

2.1. Filling materials

The aim of this study was to determine the optimal materials for 3D printing, investigating two variations of asphalt binder alongside two waste materials: waste glass and rubber tire powder. The asphalt binders evaluated were PG 58–22 (referred to as AP3) and PG 64–22 (termed AP5), exhibiting penetration values of 110 and 70 dmm at 25 ℃, respectively. A detailed properties of these binders' properties is available in Table 1. To measure the suitability of waste glass and rubber tire powder as alternatives, thus reducing asphalt binder usage, varying proportions of these waste materials (ranging from 10 % to 50 % in relation to the weight of asphalt binder) were combined with the binder. Before incorporation, both waste materials underwent sieving to achieve a particle size of 0.6 mm, in line with AASHTO T 27 guidelines [31]. This sizing decision aligned with the nozzle dimensions of the printer, set at 2 mm, requiring the waste material size to be less than 0.6 mm. The density of waste glass measured at 1.93 g/cm^3, and Table 2 provides the aggregate size distribution details for the waste glass for reference.

In addition, rubber tire powder was modified with asphalt binder as filling material in 3D printing process. The particle size of rubber tire

Table 1
Specification of two asphalt binders.

Specification	PG 58-22 (AP3)	PG 64-22 (AP5)	Test method
Specific Gravity	1.037	1.039	AASHTO T 228
Absolute Viscosity at 60 ℃, Poises	1120	2030	AASHTO T 202
Penetration at 25 ℃, dmm	110	70	AASHTO T 40

Table 2
Size gradation of waste glass.

Sieve size (mm)	4.75	2.36	1.18	0.6	0.425	0.3	0.15	0.075
Passing (%)	100	100	100	55.34	41.68	24.30	8.65	1.69

powder ranged from 0.1 to 0.6 mm as shown in Fig. 1. The specific gravity of tire powder was 1.12 g/cm^3. The result of energy-dispersive X-ray spectroscopy are shown in Table 3.

During the preparation of the asphalt binder mixture, the asphalt and waste aggregates underwent heating in an oven at 150 ℃ for a duration of two hours [15]. Subsequently, the binder was amalgamated with waste materials following the process illustrated in Fig. 1. The aim of incorporating waste materials such as waste glass and rubber tire powder was to serve as filler material, reducing the necessity for binder. To achieve this, the mixing speed and duration were regulated at 120 RPM for 5 min, respectively. Subsequent to this mixing, the resulting blend underwent an additional 30 min of heating in the oven before being poured into the section of the 3D printer designed for the binder. The specific composition of the binder mixture employed in this study is detailed in Table 4.

2.2. Development of asphalt 3D printer

Using a hot-end heating extruder integrated into the existing frame of a 3D Delta frame printer, the crack was effectively filled with the asphalt binder mixture. To achieve this seamless integration, various components were designed using the SolidWorks program [32] and subsequently 3D printed using 3D printer, as illustrated in Fig. 2. For this experiment, the binder container was crafted from 2-mm thick stainless steel, while the nozzle was made from aluminum. To ensure precise temperature control, the binder container's temperature was set at 120 ℃ for both AP3 and AP5 asphalt binder, respectively. Both the binder container and the 2 mm-nozzle were covered with a heating pad and controlled by a temperature controller. The extruder featured a DC motor with a reduction ratio of 1/200, generating a powerful shear force of up to 60 Nm for screw rotation. To manage the flowing speed of the asphalt binder mixture, the motor speed was carefully regulated using a speed controller.

Precise nozzle movement control was a crucial aspect of this study. To begin, the crack was designed in a 3D software such as SolidWorks, ensuring accurate representation. Subsequently, the 3D crack design was converted into a 3D printing file format (*. STL) and further processed using the Cura program [33]. The Cura program served as the intermediary to transform the 3D object into GCode, a language that the 3D printer reads and interprets to execute the printing process. Additionally, the program facilitated meticulous management of the object's layer-by-layer sliding, allowing for moving control over the flow of the binder material. Based on the previous research, the printing speed was controlled at 100 mm/min [16]. The sequential process of filling the crack with the binder material is visually depicted in Fig. 3, providing a clear representation of the crack-filled sample procedure.

3. Test methods

3.1. Semi-circular bending test

This test aims to evaluate the effect of different crack filled materials through 3D printing techniques as well as determine the optimum contents of waste material when incorporating with asphalt binder. A series of pre-crack semicircular bending samples were prepared based on hot mix asphalt mixture of 13 mm of Nominal Maximum Aggregate Size (NMAS). The process began by preparing cylindrical samples with a diameter of 150 mm and a height of 110 mm, which were meticulously compacted to maintain a precise 7 ± 1 % density, utilizing the Superpave Gyratory Compactor. After an initial 48-hour curing period at room temperature, the cylindrical samples were cut into semi-circular

Fig. 1. Asphalt binder mixing process.

Table 3
Chemical properties of rubber tire powder.

Components	Carbon	Oxygen	Zinc	Sulfur	Silicon	Magnesium	Aluminum
Percentages	87.9 %	8-6 %	1-7.5 %	1-1.5 %	0-3.5 %	0.15 %	0.05 %

Table 4
Proportion of binder mixtures.

Test	Waste glass modified binder	Rubber tire powder modified binder
Semi-circular bending	10 %, 20 %, 30 %, 40 %, 50 %	10 %, 20 %, 30 %, 40 %, 50 %
Shear bond strength	AP3, AP5, AP3W20, AP5W10	AP3, AP5, AP3R30, AP5R20
Four-point bending		
Binder flow rate		

Note: "AP5W-10": AP5=AP5 binder, W=waste glass, 10=10 % waste materials; "AP3R-20": AP3=AP3 binder, R=rubber tire powder, 20=20 % waste materials

bending samples, each having a 50 mm thickness [34]. At the midpoint of each semi-circular sample, an artificial crack measuring 2 mm wide and 2 mm deep was carefully created as displayed in Fig. 4. To ensure the elimination of moisture resulting from the cutting process, the samples underwent additional curing at 25 ℃. Following this, the cracked samples were subjected to filling using a specialized 3D printing machine, as exemplified in the accompanying Fig. 2b. This allowed for an assessment of the crack filling efficacy through the 3D printing process, while simultaneously investigating the optimal waste content suitable for crack filling applications.

Before conducting the semi-circular bending (SCB) test, the crack-filled samples underwent a 24-hour conditioning period at room temperature, adhering to AASHTO TP-105–13 2019 guidelines [34]. The SCB test was conducted under controlled conditions at 25 ± 1 ℃, employing a loading rate of 5 ± 0.1 mm/min and a contact load of 0.05 kN, as depicted in Fig. 5. Continuous monitoring and recording of load and deformation data occurred throughout the test duration. The evaluation of the crack-filled samples' indirect tensile strength involved a specific calculation: dividing the maximum tensile load at the failure point by the asphalt sample's cross-sectional area, following Eq. (1). Additionally, the study assessed the fracture energy of these samples, which shows material's capacity to absorb energy during fracture or failure. Determining the fracture energy was achieved by computing the area under the load-displacement curve, as outlined in Eq. (2). This comprehensive analysis offered an in-depth understanding of the crack-filled samples' behavior during the SCB test, shedding light on their tensile strength and energy absorption properties of crack-filled samples.

$$S_t = \frac{2P}{\pi D t} \tag{1}$$

Where,
S_t: indirect tensile strength (Pa),
P_{max}: peak load (N),
D: diameter of sample (m),
t: thickness of sample (m).

$$G_f = \frac{W_f}{A_{lig}} \tag{2}$$

Where,
G_f: fracture energy (J/m^2),
W_f: work of fracture (J),
A_{lig}: ligament area (m^2).

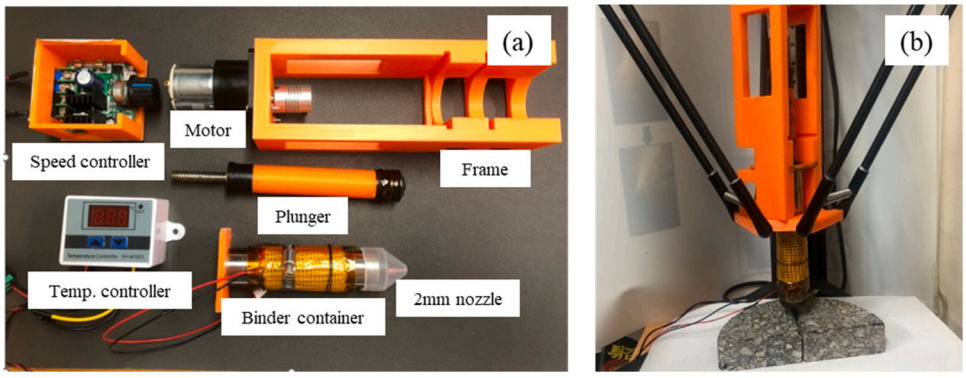

Fig. 2. Developed 3D printer parts (a) and 3D printer for asphalt binder mixtures (b).

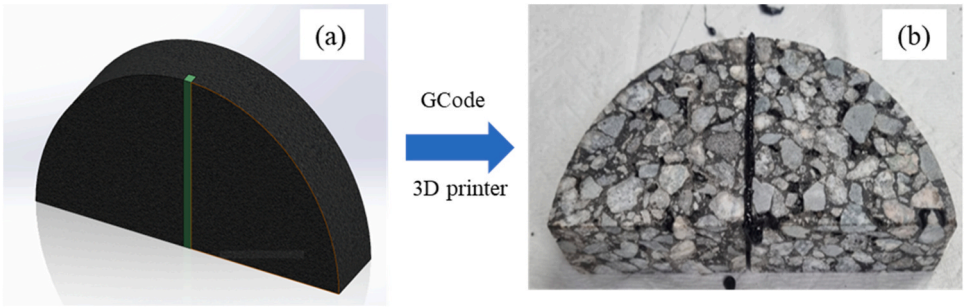

Fig. 3. Construct crack in 3D program (a) and crack filled sample by 3D printer (b).

Fig. 4. Semi-circular bending sample preparation.

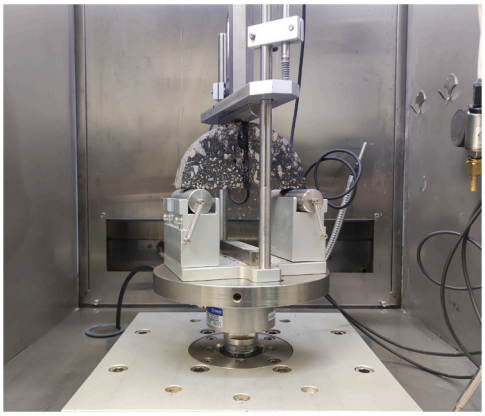

Fig. 5. Semi-circular test set up.

3.2. Shear bond strength test

In order to determine the adhesive strength of the binder mixture and asphalt concrete, a thorough shear bonding strength test was conducted using a specialized two-species cylindrical sample configuration (Fig. 6). The primary objective of this test was to assess the binder's adhesive capacity within the cracks and its ability to effectively hold the cracks together. Two distinct sample types were considered. The first involved connecting two separate cylindrical samples using the asphalt binder mixture, labeled as "2P". Each of these cylindrical samples had dimensions of 100 mm in diameter and 50 mm in height. The second sample type, known as "1P", comprised a single 100 mm-cylindrical sample that was cut in the middle and subsequently filled with the asphalt binder mixture, resulting in a height of 102 mm. The setup for both sample types is presented in Fig. 6. After filling the cracks using the 3D printing machine, the samples were conditioned in a temperature incubator at 25 ± 1 ℃ for a period of three hours prior to conducting the shear bond strength test. The test, which was based on TEX-249-F standards, was performed at a controlled loading rate of 5 mm/min and a constant temperature of 25 ± 1 ℃ [35]. To prevent sticking to the jig, the samples were covered with tape, and the interlayer was strategically positioned in the middle of the jig. Throughout the test, precise records of load displacement were meticulously documented, allowing for the subsequent calculation of the shear bond strength using Eq. (3). This comprehensive testing procedure enabled the evaluation of the adhesive capabilities of the binder mixture and its effectiveness in reinforcing and bonding cracks, providing valuable insights into the material's performance.

$$S_{max} = \frac{4P_{max}}{\pi D^2} \quad (3)$$

Where,

S_{max}: shear bond strength (Pa),
P_{max}: peak load (N),
D: diameter of sample (m).

3.3. Four-point bending test

The primary objective of the four-point bending test is to assess the impact of the 3D crack filling method on the fatigue cracking resistance of asphalt mixtures under repeated loads. The air void content of the beam sample was maintained at 7 ± 1 % [36]. To achieve this target, the weight of the mixture was adjusted based on the sample's volume and slab sample density. The slab mold, depicted in Fig. 7, had dimensions of 250 mm in width, 500 mm in length, and 50 mm in thickness. Before cutting, the slab sample underwent 24 h of conditioning. From the slab sample, three beam samples were cut, each measuring 50 mm in width, 50 mm in height, and 380 mm in length. At the center of the beam sample, an artificial crack was prepared, featuring a notch with dimensions of 3 mm in width and 5 mm in depth, running from the front to the back of the sample. Subsequently, the beam samples were left to dry for 72 h prior to testing. In order to minimize the preparation workload, the optimal combination of waste materials and binder identified through the Semi-circular bending test was chosen for the subsequent four-point bending test.

To ensure an equivalent temperature distribution, the beam samples were conditioned in a temperature incubator at 25 ± 1 ℃ for three hours. The test was conducted in accordance with AASHTO T 321 under controlled stress mode, as illustrated in Fig. 7. A haversine load waveform, with a magnitude of 0.7 kN and a frequency of 5 Hz, was applied during the testing process. The contact sitting load was maintained at 0.035 kN. The test was carried out until reaching either 2500 cycles or 10 mm of permanent deformation, whichever occurred first. Throughout the testing process, the number of loading cycles and deformation were continuously recorded for analysis and evaluation.

3.4. Flow test of binder mixture

To evaluate the impact of temperature on the flow behavior of the binder-aggregate mixture, the binder flow rate was measured. This investigation involved two types of binder as well as the optimized combination of waste materials and binder mixture. Fig. 8 outlines the experimental sequence: initially, the binder-aggregate mixtures were prepared and heated in an oven for 30 min. Subsequently, the heated binder blend was poured into the binder container within a 3D printer. To reach the desired temperature of 120 ℃, a heating pad was employed to further heat the binder container. Evaluating the binder flow rate entailed pumping the binder-aggregate mixture with a constant motor rotation set at 60 RPM for a duration of 15 s. The weight of the binder

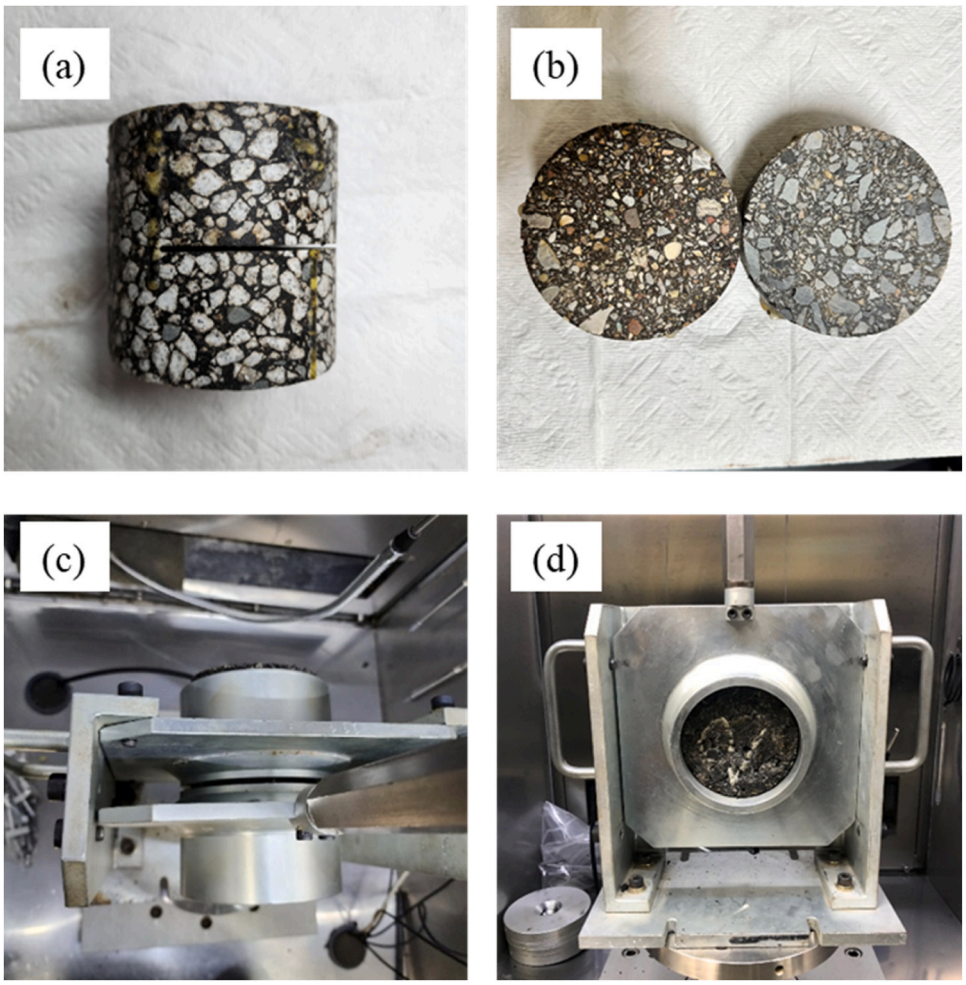

Fig. 6. Type 1P sample (a), Type 2P sample, top view (c), and front view (d).

was recorded, and the binder flow rate was determined through the application of Eq. (4).

$$BR = \frac{W}{\Delta t} \tag{4}$$

Where,

BR: binder flow rate (gram/second),
W: weight of binder (gram),
Δt: time to pump (15 s).

4. Results and discussion

4.1. Semi-circular bending test

Fig. 9 displays the indirect tensile strength (ITS) of crack-filled samples. Overall, the 3D printing method for crack filling exhibited a higher ITS compared to the control samples (NoFill sample). The untreated control sample displayed the lowest ITS at 312 kPa. Conversely, the crack-filled samples demonstrated a substantial enhancement, achieving a 42 % increase in indirect tensile strength compared to the unfilled control sample. Notably, waste glass-modified asphalt binders such as AP5W10 and AP3W20 exhibited ITS values of 428 kPa and 416 kPa, respectively. Similarly, samples filled with rubber-modified asphalt binder also demonstrated improved ITS, such as AP3R30 and AP5R20, recording strengths of 430 kPa and 419 kPa, respectively. The incorporation of waste materials (e.g., waste glass, tire powder) remarkably improved the ITS when compared to samples filled by pure binder. Waste material modified AP5 binder showed an approximate 10 % improvement, while AP3 binder showcased a substantial 21 % enhancement compared to AP5 and AP3 pure binder, respectively. This enhancement was attributed to the presence of waste material in the binder, reinforcing the structure of the modified binder and subsequently increasing the internal frictional forces between aggregates. However, a higher concentration of waste materials strongly reduced the ITS of the crack-filled sample. For instance, as depicted in Fig. 8, the ITS of the AP3R40 sample only reached 329 kPa, displaying minimal improvement compared to the control sample. This was due to the rapid drying of the binder after nozzle emission, failing to effectively connect both sides of the cracks and hence reducing the efficacy of crack filling. Particularly concerning mixtures modified with rubber tire powder, an incorporation exceeding 40 % by weight resulted in high viscosity, preventing the binder mixture from flowing out of the nozzle. Similarly, utilizing more than 30 % waste glass was not advisable due to binder and waste glass segregation resulting from their differing densities, causing the waste glass to accumulate at the container bottom. This excessive aggregate in the asphalt binder mixture also led to reduced cohesion between aggregate and binder, diminishing resistance to bearing force.

Fig. 10 exhibits the load-deformation characteristics of control sample and four crack-filled samples employing the 3D printing method. The unfilled control sample, lacking sealing, displayed brittle behavior with a deformation of 0.79 mm at peak load, ultimately reaching a maximum deformation of 2.00 mm. This brittleness can be attributed to the artificial crack introduced during the preparation process, leading the sample to be more susceptible to failure. In contrast, the crack-filled

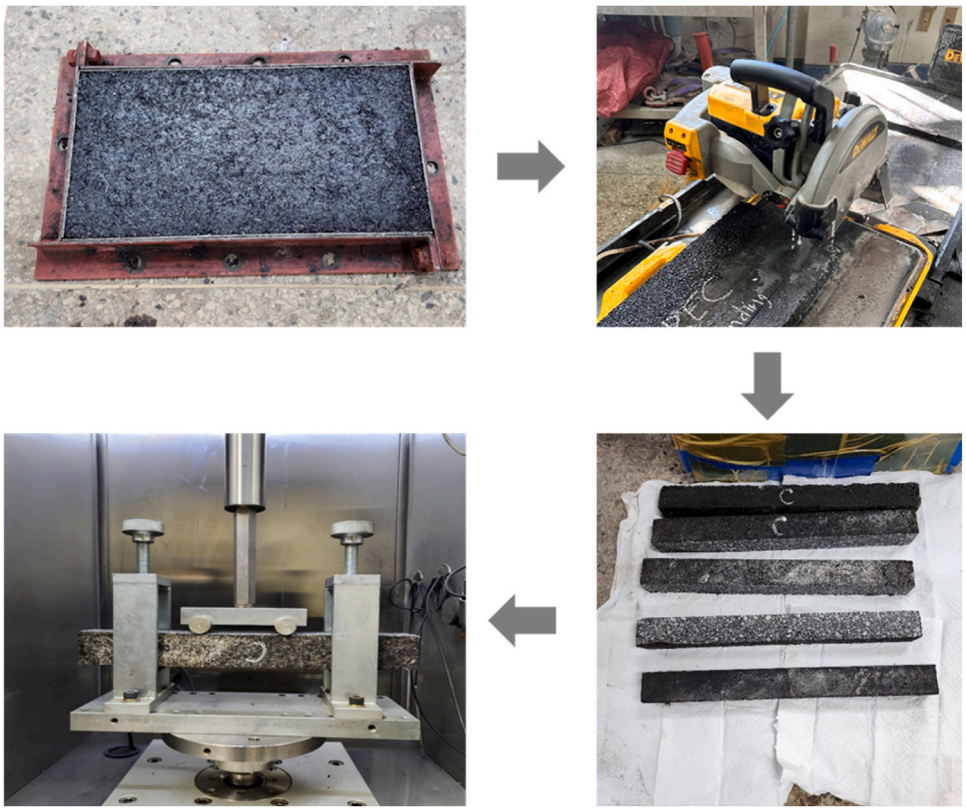

Fig. 7. Preparation of beam sample and four point bending test set up.

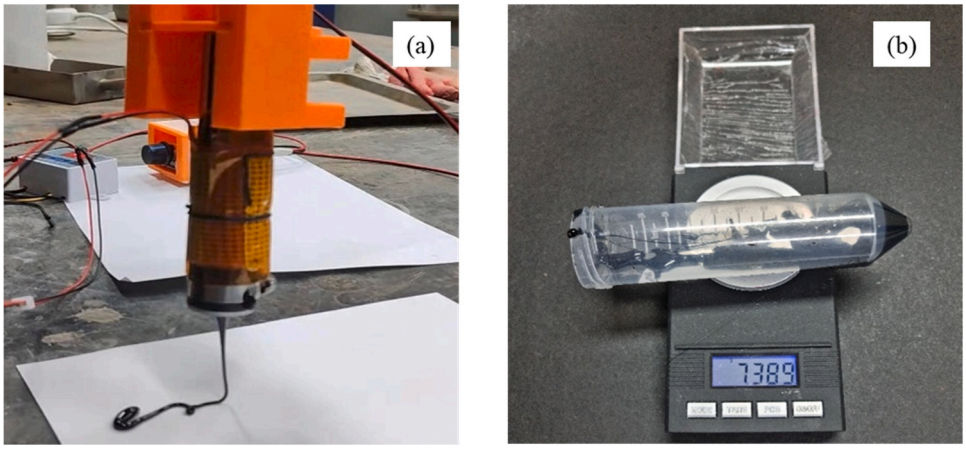

Fig. 8. Binder flow test (a) and measure weight of binder aggregate (b).

samples demonstrated significantly greater deformation at peak load, recording twice the deformation compared to the control sample. For instance, the AP5W10 mixture and AP3W20 displayed peak load deformations of 2.14 mm and 2.08 mm, respectively. The material used for crack filling functions as a bridge between crack surfaces, increasing support and cohesion within the asphalt sample. Additionally, it acts as a crack-arresting agent, impeding further crack propagation. When the crack encounters this filling material, it encounters increased resistance, resulting in a more ductile mode of failure. Notably, asphalt binder modified with rubber tire powder exhibited the highest deformation, with AP3R30 and AP5R20 presenting deformations of 2.35 mm and 2.31 mm at peak load, respectively. Specifically, samples filled with rubber tire powder displayed greater post-peak ductility compared to those filled with waste glass materials. This disparity might be attributed to the modified materials' effect; the rubber tire powder potentially stiffened the binder during the mixing process, resulting in a stiffer binder. Conversely, waste glass primarily functions as an aggregate, not significantly impacting the stiffness of the asphalt binder.

Fig. 11 illustrates the fracture energy exhibited by both the crack-filled and control samples. This parameter serves as a key indicator of the load-displacement behavior and resistance against cracking. A higher fracture energy value denotes a stronger resistance to cracking. Overall, the crack-filled samples demonstrated fracture energy values roughly 2–3 times higher than those of the unfilled control samples. For instance, the control sample exhibited a fracture energy of 1293 J/m^2, while samples filled with original AP3 and AP5 recorded fracture energies of 2159 J/m^2 and 2596 J/m^2, respectively. The variance in fracture energy between AP3 and AP5 can be attributed to the differing

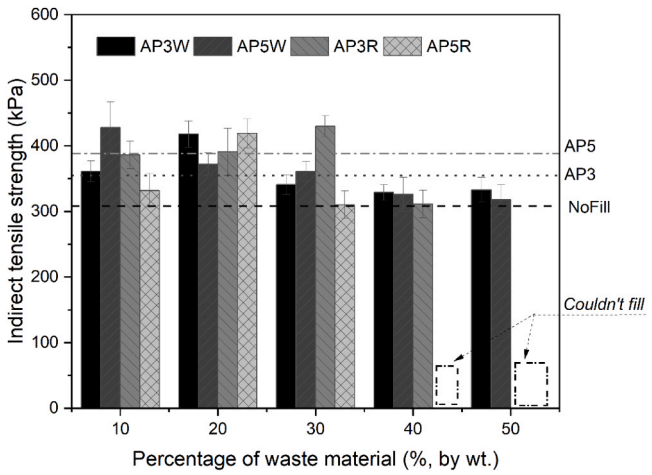

Fig. 9. Indirect tensile strength of crack filled sample.

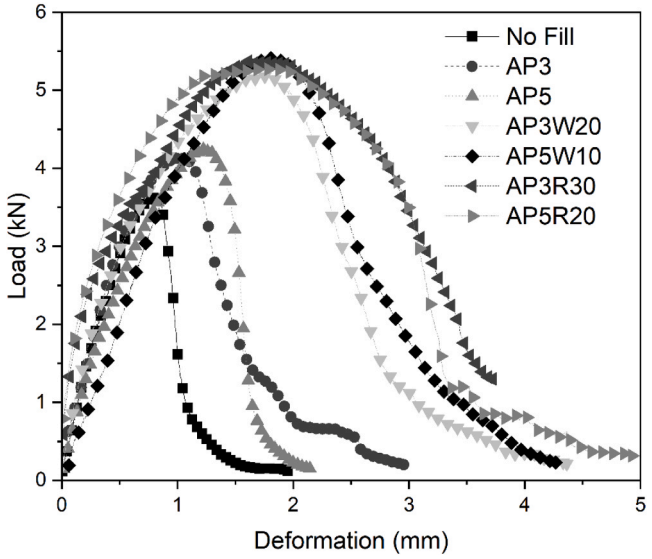

Fig. 10. Load and deformation behavior.

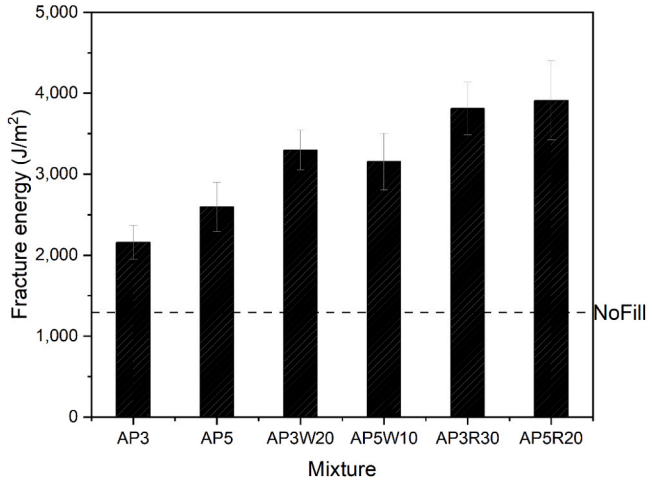

Fig. 11. Fracture energy of filled mixtures.

viscosities of their binders. Among the crack-filled samples, the AP5R20 mixture displayed the highest fracture energy at 3910 J/m^2. This heightened fracture resistance in the crack-filled samples is credited to the sealing effect of the binder mixture, contributing to increased peak load and deformation in these samples, thereby enhancing their overall performance under bending conditions. The significantly increased fracture energy values observed in the crack-filled samples underscore their superior ability to withstand cracking, offering valuable insights for evaluating their potential practical applications.

4.2. Shear bond strength test

As shown in Fig. 12, the shear bond strength test results demonstrate that the AP5 binder exhibits higher shear bond bending strength than the AP3 binder. Specifically, "1P" samples filled with asphalt binder original AP5 displayed approximately 11 % higher shear bond strength compared to those with original AP3. Notably, the highest shear bond strength of 421 kPa and 411 kPa were achieved in samples filled with mixture AP5W10 and AP5R20. In addition, samples containing AP3W20 and AP3R30 reached shear bond strength of 406 kPa and 394 kPa, respectively. This indicates that the AP5 binder grade outperforms AP3 in terms of shear bonding strength, likely due to its higher viscosity, resulting in improved bonding and higher shear bond bending strength.

Moreover, incorporation of waste materials in asphalt binder for crack fill can restore approximately 18–36 % shear bond strength as shown in sample 1P-NoFill, 1P-AP5W10, and 1P-AP3R30, respectively. This can be explained by the presence of filled materials (e.g., binder, waste glass, rubber tire powder) can fill the voids in the cracks and therefore create a larger contact area. In addition, filling the crack with a filling material (e.g., rubber tire powder modified binder and waste glass modified asphalt binder), the stress concentration at the crack tip is reduced. This redistribution of stress helps to prevent localized failure, enhancing the overall shear bond strength. These factors collectively contribute to better bonding and mechanical properties, resulting in higher shear bond strength values for the crack-filled sample. An interesting finding in this study is that incorporating waste glass and rubber tire powder into the binder leads to a significant increase in shear bond strength, approximately 15 % for AP5 and 9 % for AP3 binder mixtures. This enhancement can be attributed to the interlocking forces between waste materials, which effectively resist the shear forces during testing. Waste glass particles tend to interlock with each other, adding stability and resisting crack propagation during the shear bond strength test. Consequently, the inclusion of waste glass in the binder mixture contributes to the overall increase in shear bond strength compared to samples without waste glass.

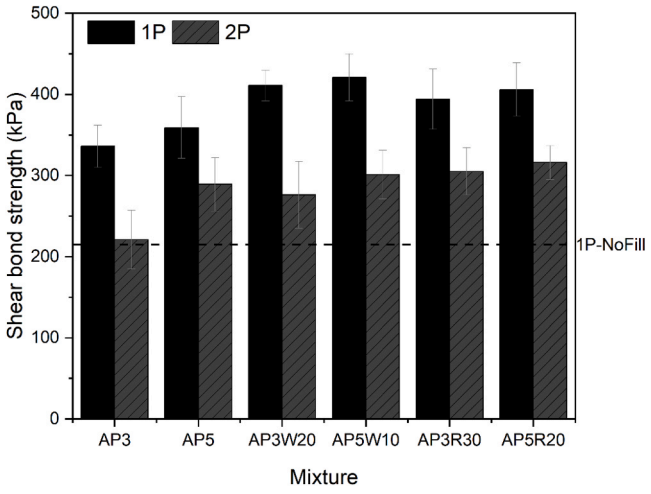

Fig. 12. Shear bond strength of crack filled samples.

4.3. Four-point bending test

The four-point bending test results, displayed in Fig. 13, reveal valuable insights regarding the performance of crack-filled samples compared to samples without binder filling over 1500 loading cycles. Notably, the crack-filled samples exhibit lower permanent deformation, indicating their enhanced resistance to deformation. Upon analysis, it becomes evident that the NoFill (Control) mixture displayed the highest permanent deformation, reaching 10 mm after 598 loading cycles. Moreover, the deformation of the control sample followed a linear behavior, with an approximate deform rate of 1.67 mm per 100 load cycles. In contrast, the incorporation of waste materials (e.g., waste glass and rubber tire powder) through 3D printing techniques significantly improved the deformation resistance of the samples. For example, samples filled with original asphalt binders (AP3 and AP5) demonstrated lower deformation values compared to the control sample, with the terminated cycles of 1072 and 1355 cycles, respectively. Particularly remarkable was the performance of samples filled with binder mixture AP5W10 and AP5R20, which exhibited the highest number of cycles. As shown in Fig. 9, the sample filled by AP5W10 and AP5R20 binder mixture experienced 10 mm of deformation after 1504 and 1752 loading cycles, with deformation rates of 0.67 mm and 0.57 mm per 100 cycles, respectively. This phenomenon can be attributed to several key factors. Firstly, the presence of filler material within the crack effectively bridges the gap and prevents further opening of the crack, resulting in reduced deflection under the applied load and consequently lower deformation. Secondly, the filler material facilitates a more even distribution of the load across the beam, leading to enhanced deformation resistance in the crack-filled samples. In general, these findings underscore the effectiveness of incorporating waste materials, such as waste glass and rubber tire powder, in crack-filled samples to improve their mechanical performance. The enhanced resistance to permanent deformation observed in the crack-filled samples holds promising implications for the development of more durable and resilient materials in structural engineering and construction applications. Further exploration and utilization of 3D printing techniques with suitable filler materials could pave the way for innovative and efficient solutions in engineering design and infrastructure development.

4.4. Flow test of binder mixture

Fig. 14 illustrates the flow rate outcomes for a binder aggregate mixture at various content of waste materials. Generally, the addition of waste material could lightly reduce the flow rate of asphalt binder. The

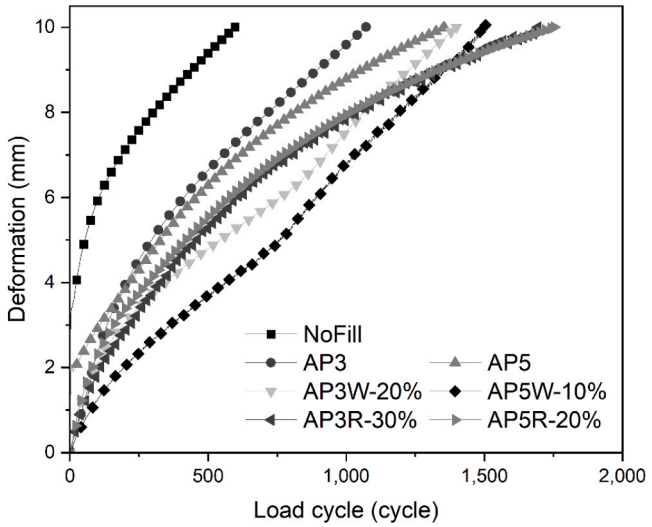

Fig. 13. Four-point bending result of crack filled sample.

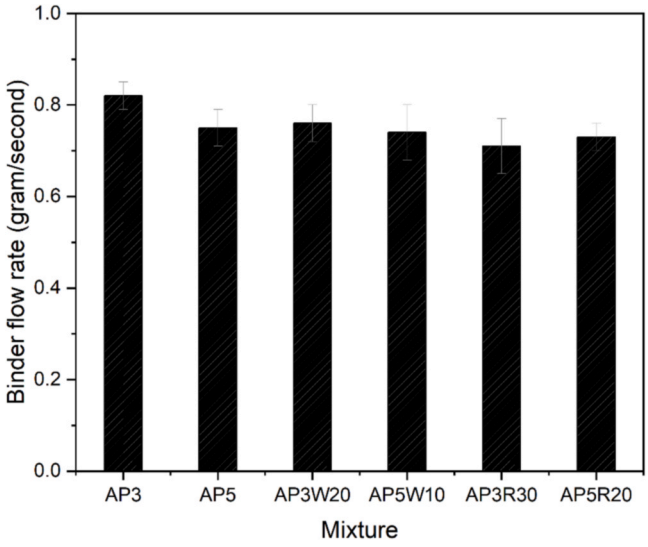

Fig. 14. Binder flow rate.

AP3 binder acquired the highest flow rate, which was 0.82 g/s compared to 0.75 g/s of original AP5. This was obviously due to the difference in binder rate, AP3 was lower viscosity than AP5. Although AP3 presents a higher flow rate, the addition of 30 % rubber tire powder presented the lowest binder flow rate of 0.71 g/s. To ensure the 3D printing potential, it is essential for the printing material not to be excessively liquid. Therefore, this study employed temperatures of 120 ℃ instead of 150 ℃ when mixing the binder with aggregates. By using a printing material with an appropriate viscosity, the aggregates, such as waste glass and rubber tire powder, can be adequately held within the material's structure. Additionally, higher heating temperatures tend to liquefy the binder, causing it to flow automatically out of the nozzle under the influence of gravity. Moreover, the presence of high-density aggregates, like waste glass, also influenced the binder flow rates. While higher heating temperatures may reduce asphalt binder viscosity, resulting in higher flow rates, it may also lead to segregation of the binder and aggregate. As aggregates possess a higher specific gravity than the asphalt binder, they tend to accumulate at the container's bottom due to gravity. Consequently, an appropriate viscosity of the binder is necessary to retain the aggregates as they flow out of the nozzle. Considering these findings, it is recommended to use AP5 with 10 % waste glass and AP5 with 20 % rubber tire powder for the 3D crack filling process.

5. Conclusions

The objective of this study is to utilize waste materials such as waste glass and rubber tire powder as replacement asphalt binder in pavement crack sealing through a three-dimensional (3D) printing technology. The primary focus is to minimize binder consumption and make use of waste glass and rubber tire powder as printing materials. The optimal amount of waste material in the modified asphalt binder was determined through shear point bending tests. Furthermore, the performance of the crack-filled samples was assessed using semi-circular bending and four-point bending tests. These tests were conducted to evaluate the effectiveness of the 3D crack sealing method in terms of recovering strength under both monotonic and repeated loads. The following key findings emerged from this research:

- 3D printing for crack filling significantly improved indirect tensile strength (ITS), showing up to a 42 % enhancement compared to unfilled samples. Filling materials like AP5 with 90 % binder and 10 % waste glass, or AP5 with 80 % binder and 20 % rubber tire powder,

exhibited the highest ITS. However, increasing waste glass content reduced ITS.

- Crack-filled samples demonstrated better ductility, deforming roughly twice as much as unfilled samples at peak load, due to the crack-sealing material acting as a cohesive bridge.
- Crack-filled samples showed about double the fracture energy of unfilled samples, with mixtures containing 10 % waste glass or 20 % rubber tire powder showing the highest fracture resistance. This improvement was attributed to the binder mixture's sealing effect.
- AP5 binder exhibited superior shear bond bending strength compared to AP3. Incorporating waste materials (10 % waste glass or 20 % rubber tire powder) significantly boosted shear bond strength due to improved interlocking forces.
- Filler material through 3D printing notably reduced permanent deformation, preventing crack expansion. However, caution is advised against using over 40 % rubber tire powder at 120 ℃ due to increased binder viscosity. Control of heating temperature is crucial for high-density materials like waste glass to prevent segregation.

The current study has evaluated the performance of waste glass and rubber tire powder as pavement crack filling materials throughout 3D technology. However, to achieve a fully automated crack filling process using 3D technology, it is essential to further investigate and develop automated crack or pothole detection methods. This would contribute to the complete automation of crack filling using 3D technology.

CRediT authorship contribution statement

Phan Tam Minh: Writing – review & editing, Writing – original draft, Software, Methodology, Formal analysis, Data curation, Conceptualization. **Ma Hye-Ju:** Writing – original draft, Visualization, Formal analysis, Data curation. **Park Dae-Wook:** Writing – review & editing, Supervision, Project administration, Methodology.

Declaration of Competing Interest

The authors whose names are listed immediately below certify that they have NO affiliations with or involvement in any organization or entity with any financial interest or non-financial interest in the subject matter or materials discussed in this manuscript.

Data availability

Data will be made available on request.

Acknowledgements

This work was supported by the National Research Foundation of Korea (NRF) grant funded by the Korea government (MSIT) (No. NRF-2022R1F1A1063979).

References

[1] M.R. Islam, R.A. Tarefder, Pavement Design: Materials. Analysis, and Highways, McGraw Hill, 2020.
[2] E.R. Brown, P.S. Kandhal, F.L. Roberts, Y.R. Kim, D.-Y. Lee, T.W. Kennedy. Hot mix asphalt materials, mixture design, and construction, 2009.
[3] J.G. Speight, Asphalt Materials Science and Technology, Elsevier Inc., 2015.
[4] T.M. Phan, T.H.M. Le, D.-W. Park, Evaluation of cracking resistance of healed warm mix asphalt based on air-void and binder content, Road. Mater. Pavement Des. (2020), https://doi.org/10.1080/14680629.2020.1829010.
[5] Y. Fang, B. Ma, K. Wei, X. Wang, X. Kang, F. Liu, Performance of single-component epoxy resin for crack repair of asphalt pavement, Constr. Build. Mater. 304 (2021) 124625, https://doi.org/10.1016/j.conbuildmat.2021.124625.
[6] T.M. Phan, D.-W. Park, T.H.M. Le, Crack healing performance of hot mix asphalt containing steel slag by microwaves heating, Constr. Build. Mater. 180 (2018) 503–511, https://doi.org/10.1016/j.conbuildmat.2018.05.278.
[7] Kyle P. Kwiatkowski, S.O. Irina, ter M. Herbert, H. Andreas, C. Paul, G.P.M. R. Dewulf, Modeling cost impacts and adaptation of freeze–thaw climate change on a porous asphalt road network, J. Infrastruct. Syst. 26 (2020) 4020022, https://doi.org/10.1061/(ASCE)IS.1943-555X.0000559.
[8] P. Cong, Z. Chen, W. Ge, Influence of moisture on the migration of asphalt components and the adhesion between asphalt binder and aggregate, Constr. Build. Mater. 385 (2023) 131513, https://doi.org/10.1016/j.conbuildmat.2023.131513.
[9] H. Goli, M. Latifi, Evaluation of the effect of moisture on behavior of warm mix asphalt (WMA) mixtures containing recycled asphalt pavement (RAP), Constr. Build. Mater. 247 (2020) 118526, https://doi.org/10.1016/j.conbuildmat.2020.118526.
[10] X. Chen, H. Wang, G. Venkiteela, Asphalt Pavement Pothole Repair Using the Pre-Heating Method: An Integrated Experiment and Modeling Study, Transp. Res. Rec. 0 (n.d.) 03611981231164066. https://doi.org/10.1177/03611981231164066.
[11] F. Gong, X. Cheng, Y. Chen, Y. Liu, Z. You, 3D printed rubber modified asphalt as sustainable material in pavement maintenance, Constr. Build. Mater. 354 (2022) 129160, https://doi.org/10.1016/j.conbuildmat.2022.129160.
[12] Y. Tan, M. Guo, L. Cao, L. Zhang, Performance optimization of composite modified asphalt sealant based on rheological behavior, Constr. Build. Mater. 47 (2013) 799–805, https://doi.org/10.1016/j.conbuildmat.2013.05.015.
[13] G. Ma, L. Wang, Y. Ju, State-of-the-art of 3D printing technology of cementitious material—an emerging technique for construction, Sci. China Technol. Sci. 61 (2018) 475–495, https://doi.org/10.1007/s11431-016-9077-7.
[14] R. Comminal, W.R. Leal da Silva, T.J. Andersen, H. Stang, J. Spangenberg, Modelling of 3D concrete printing based on computational fluid dynamics, Cem. Concr. Res. 138 (2020) 106256, https://doi.org/10.1016/j.cemconres.2020.106256.
[15] J. Liu, X. Yang, X. Wang, J.W. Yam, A laboratory prototype of automatic pavement crack sealing based on a modified 3D printer, Int. J. Pavement Eng. 23 (2022) 2969–2980, https://doi.org/10.1080/10298436.2021.1875225.
[16] F.K.A. Awuah, A. Garcia-Hernández, Machine-filling of cracks in asphalt concrete, Autom. Constr. 141 (2022) 104463, https://doi.org/10.1016/j.autcon.2022.104463.
[17] E. Bocci, E. Prosperi, Recyclability of reclaimed asphalt rubber pavement, Constr. Build. Mater. 403 (2023) 133040, https://doi.org/10.1016/j.conbuildmat.2023.133040.
[18] D.E. Ewa, J.O. Ukpata, G.A. Akeke, A.A. Etika, E.I. Adah, Use of waste glass fines to improve rigidity ratio of asphalt, Cogent Eng. 9 (2022) 2107197, https://doi.org/10.1080/23311916.2022.2107197.
[19] A. Ivica, M. Ivan, Influence of compaction energy on volumetric properties of hot-mix asphalt with waste glass content, J. Mater. Civ. Eng. 31 (2019) 4019241, https://doi.org/10.1061/(ASCE)MT.1943-5533.0002887.
[20] C.M. J, W.Y. D, Porous asphalt mixture with a combination of solid waste aggregates, J. Mater. Civ. Eng. 27 (2015) 4014194, https://doi.org/10.1061/(ASCE)MT.1943-5533.0001154.
[21] S. Kalampokis, D. Kalama, F. Kesikidou, M. Stefanidou, E. Manthos, Assessment of waste glass incorporation in asphalt concrete for surface layer construction, Materials (Basel) 16 (2023), https://doi.org/10.3390/ma16144938.
[22] F.E. H, O.D. J, A.-L. Taher, Synthesis and characterization of biomodified rubber asphalt: sustainable waste management solution for scrap tire and swine manure, J. Environ. Eng. 139 (2013) 1454–1461, https://doi.org/10.1061/(ASCE)EE.1943-7870.0000765.
[23] Munirwansyah Hamzani, M. Hasan, S. Sugiarto, Determining the properties of semi-flexible pavement using waste tire rubber powder and natural zeolite, Constr. Build. Mater. 266 (2021) 121199, https://doi.org/10.1016/j.conbuildmat.2020.121199.
[24] X. Li, J. Li, J. Wang, J. Yuan, F. Jiang, X. Yu, F. Xiao, Recent applications and developments of Polyurethane materials in pavement engineering, Constr. Build. Mater. 304 (2021) 124639, https://doi.org/10.1016/j.conbuildmat.2021.124639.
[25] W. Lan, X. Yong-ming, C. Chun-qing, Experimental Studies on Microstructure and Technical Performance of Multiphase Compound Crumb Rubber Modified Asphalt, ICCTP 2010 (2012) 2920–2926, https://doi.org/10.1061/41127(382)310.
[26] M.M. Khabiri, A. Khishdari, E. Gheibi, Effect of tyre powder penetration on stress and stability of the road embankments, Road. Mater. Pavement Des. 18 (2017) 966–979, https://doi.org/10.1080/14680629.2016.1194879.
[27] A. Kumar, R. Choudhary, A. Kumar, Characterisation of asphalt binder modified with ethylene–propylene–diene–monomer (EPDM) rubber waste from automobile industry, Road. Mater. Pavement Des. 22 (2021) 2044–2068, https://doi.org/10.1080/14680629.2020.1740772.
[28] M. Liang, X. Xin, W. Fan, S. Ren, J. Shi, H. Luo, Thermo-stability and aging performance of modified asphalt with crumb rubber activated by microwave and TOR, Mater. Des. 127 (2017) 84–96, https://doi.org/10.1016/j.matdes.2017.04.060.
[29] H. Yu, Z. Zhu, Z. Leng, C. Wu, Z. Zhang, D. Wang, M. Oeser, Effect of mixing sequence on asphalt mixtures containing waste tire rubber and warm mix surfactants, J. Clean. Prod. 246 (2020) 119008, https://doi.org/10.1016/j.jclepro.2019.119008.
[30] W. Zheng, H. Wang, Y. Chen, J. Ji, Z. You, Y. Zhang, A review on compatibility between crumb rubber and asphalt binder, Constr. Build. Mater. 297 (2021) 123820, https://doi.org/10.1016/j.conbuildmat.2021.123820.
[31] AASHTO T 27, Standard Method of Test for Sieve Analysis of Fine and Coarse Aggregates, (2022).
[32] SolidWorks Corp., SOLIDWORKS, (2022). https://www.solidworks.com/.
[33] Ultimaker, Cura, (2023). https://ultimaker.com/software/ultimaker-cura/ (accessed July 24, 2023).

[34] AASHTO TP-105–13, Method of Test for Determining the Fracture Energy of Asphalt Mixtures Using the Semicircular Bend Geometry (SCB), (2019).
[35] Texas Department of Transportation, Tex-249-F Test procedure for shear bond strength test, 2021.
[36] AASHTO T 321, Standard Method of Test for Determining the Fatigue Life of Compacted Asphalt Mixtures Subjected to Repeated Flexural Bending, 2022.